Disorder driven allosteric control of protein activity

Wei-Ven Tee [a,b], Enrico Guarnera [a,1], Igor N. Berezovsky [a,b,*]

[a] Bioinformatics Institute (BII), Agency for Science, Technology and Research (A*STAR), 30 Biopolis Street, #07-01, Matrix 138671, Singapore
[b] Department of Biological Sciences (DBS), National University of Singapore (NUS), 8 Medical Drive 117597, Singapore

ABSTRACT

Studies of protein allostery increasingly reveal an involvement of the back and forth order-disorder transitions in this mechanism of protein activity regulation. Here, we investigate the allosteric mechanisms mediated by structural disorder using the structure-based statistical mechanical model of allostery (SBSMMA) that we have previously developed. We show that SBSMMA accounts for the energetics and causality of allosteric communication underlying dimerization of the BirA biotin repressor, activation of the sortase A enzyme, and inhibition of the Rac1 GTPase. Using the SBSMMA, we also show that introducing structural order or disorder in various regions of esterases can originate tunable allosteric modulation of the catalytic triad. On the basis of obtained results, we propose that operating with the order-disorder continuum allows one to establish an allosteric control scale for achieving desired modulation of the protein activity.

1. Introduction

Biological functions on the molecular level are orchestrated and tightly controlled by a multitude of intra- and intermolecular signaling events within a cell. A common theme underlying many signaling and regulatory mechanisms is that the functional activity of macromolecules is modulated via remote perturbations by small molecules/ligands, a pervasive phenomenon known as allostery (Guarnera and Berezovsky, 2016; Guarnera and Berezovsky, 2019). The original definition of allostery was given by Monod, Changeux, and Jacob in their seminal work in 1963 entitled "Allosteric proteins and cellular control systems" (Monod et al., 1963). The main postulates of this definition include: first, "proteins … possess two, or at least two, stereospecifically different, non-overlapping receptor sites"; second, "binding of the allosteric effector to the regulatory exosite (allosteric site) induces conformational alterations affecting activity of the regulated functional site". Recognition of the omnipresence of allosteric mechanisms in different proteins from small monomers, to large oligomeric molecular machines, and from folded globular proteins to intrinsically disordered ones have greatly expanded the paradigm of protein allostery over the past decades (Guarnera and Berezovsky, 2016; Gunasekaran et al., 2004). Investigations of allosteric mechanisms and cooperativity showed that signals originated by conformational changes and/or fluctuations are communicated between distant sites through changes in the dynamics of the structure upon binding of an effector molecule to one of these sites (Cooper and Dryden, 1984; Mitternacht and Berezovsky, 2011; Mitternacht and Berezovsky, 2011; Tsai & Nussinov, 2014), leading to a conjecture that allostery is an intrinsic property of all dynamic proteins (Gunasekaran et al., 2004; Mitternacht and Berezovsky, 2011). Frequent and potentially large contribution of inherently flexible protein regions, such as surface loops and linkers between secondary structure elements, to alteration of the structural states and to the overall protein dynamics have lead to a hypothesis on their potential involvement in allosteric mechanisms (Hilser and Thompson, 2007; Huang et al., 2020; Ma et al., 2011; Papaleo et al., 2016).

While the concept of protein intrinsic disorder was first introduced for characterizing native (pre)molten globules and random coils in poor solvents (Uversky, 2002), the current view on protein disorder is much wider, spanning from functional and regulatory disordered segments as short as few residues to fully disordered protein domains and proteins (Papaleo et al., 2016; van der Lee et al., 2014). The involvement of disorder in biological functions was coarsely classified into three broad categories: (i) targeted regulation provided by the post-translational modifications (PTMs); (ii) structure and interface formation; (iii) adaptability and variability (Gsponer and Babu, 2009). More specifically, these categories include display of the PTMs targets, molecular recognition and

structure formation, distancing and positioning of domains and oligomers, and effectors of functions or signals for complex assembly upon ligand binding or protein–protein interaction, to name a few (van der Lee et al., 2014). As a result, a uniform description and classification of protein disorder appeared to be a challenging task, making it hard to propose a universal set of characteristics for quantifying and predicting disorder, its structural-functional features, evolutionary history, and other aspects (van der Lee et al., 2014).

In this work, we focus our attention on the intrinsically disordered regions (IDRs) of proteins, which are abundant in proteomes and are known to play key roles in cellular signaling and regulation, transcriptional and translational control, and other biological processes (Dunker et al., 2008; Tokuriki et al., 2009; Wright and Dyson, 1999). Rapid developments in the field of protein disorder have generated increasing amount of evidence that points to a presence of allosteric mechanisms in regulation of protein function that involves IDRs despite the lack of well-defined three-dimensional structures (Li et al., 2017; Garcia-Pino et al., 2010; Berlow et al., 2018). It has also been shown that intrinsic disorder enhances allosteric coupling between protein domains (Hilser and Thompson, 2007; Papaleo et al., 2016) and allows modulation of allostery in a promiscuous molecular hub (Ferreon et al., 2013). The potential of engineering extrinsic local disorder to control protein activity in living cells through mutations or external factors has also been gradually recognized, as illustrated in a number of recent work (Li et al., 2017; Karginov et al., 2010; Dagliyan et al., 2016; Saavedra et al., 2018). All of the above hint that disorder can play an important role in allosteric regulation of widely defined protein functions in many more cases than it was previously found and documented. Consequently, it calls for more rigorous experimental studies and development of computational approaches that would allow to use structural disorder for inducing and tuning desired allosteric effects. In this work, the assumption is that from the structural perspective, there is no conceptual difference between intrinsically disordered regions and flexible elements, such as linkers and loops, and they may be considered as intrinsically disordered elements (van der Lee et al., 2014; Dunker et al., 2013). To this end, we are interested in exploring the allosteric effects of loosening and rigidifying of protein regions, which requires a uniform characterization of considered IDRs for the modeling of the induced order/disorder, and for quantifying their effects on the protein function. We introduced, therefore, an operational definition of protein order-disorder, which includes only structural aspect of this otherwise complex problem (Hilser and Thompson, 2007; Huang et al., 2020; Ma et al., 2011; Papaleo et al., 2016; van der Lee et al., 2014).

We have previously developed a structure-based statistical mechanical model of allostery (SBSMMA), which provides a quantitative description of the causality and allows to estimate the energetics of allosteric communication at per-residue resolution (Guarnera and Berezovsky, 2019; Guarnera and Berezovsky, 2019; Guarnera and Berezovsky, 2016). In this study, we use SBSMMA for investigating how order-to-disorder and disorder-to-order transitions work in allosteric regulation of the protein activity of BirA biotin repressor (Wang et al., 2017), sortase A enzyme (Pang and Zhou, 2015), and Rac1 GTPase (Dagliyan et al., 2016). We also explore how alteration of structural order and disorder can be used in the engineering and design of allosteric regulation in a set of esterases. We show that understanding of disorder-based allosteric mechanisms gained from the above examples allows us to propose a generic strategy for inducing tunable allosteric control of protein activity, in which disorder/order-to-order/disorder transitions play a role of perturbations (Guarnera and Berezovsky, 2019) required for inducing the allosteric signal.

2. Materials and Methods

2.1. Structure-based statistical mechanical model of allostery (SBSMMA)

The recently developed SBSMMA (Guarnera and Berezovsky, 2019; Guarnera and Berezovsky, 2019; Guarnera and Berezovsky, 2016) has

been used for quantifying the energetics of allosteric communication upon ligand binding and/or amino acid changes in the protein structure, and for identifying potential regulatory exosites through a reverse perturbation at functional sites (Tee et al., 2018). In this study, we apply the SBSMMA for investigating the allosteric effect of disorder-to-order and opposite transitions.

A single crystal structure is used to construct the Cα harmonic model for the unperturbed and perturbed states of the protein. The energy function of the unperturbed state (denoted as 0) is given by

$$E^{(0)}(\delta r) = \sum_{i,j} k_{ij} \left(d_{ij} - d_{ij}^0 \right)^2 \tag{1}$$

where δr is the 3N-dimensional vector of displacements of Cα atoms with respect to the reference structure. The d_{ij} is the distance between Cα atoms i and j and the corresponding distance in the reference structure is d_{ij}^0. The distance-dependent force constant k_{ij}, decays as $(1/d_{ij}^0)^6$ with a global distance cutoff at 25 Å (Hinsen et al., 2000). In the perturbed state P, in which n residue(s) are perturbed, $P = \{p_1, p_2, ..., p_n\}$, the force constant is altered by a scale factor α, so the corresponding energy function is

$$E^{(P)}(\delta r) = \sum_{i,j,i \notin P} k_{ij} \left(d_{ij} - d_{ij}^0 \right)^2 + \alpha \sum_{i,j,i \in P} k_{ij} \left(d_{ij} - d_{ij}^0 \right)^2. \tag{2}$$

Here, two types of perturbation are performed. Destabilizing DOWN perturbation ($P \downarrow$) is done with $\alpha = 10^{-2}$, which weakens the force constants of the interactions between the perturbed residue(s) with the neighbors, to simulate local disorder. Conversely, induced rigidity is modelled by stabilizing UP perturbation ($P \uparrow$) with $\alpha = 10^2$, which increases the force constants and strengthens the interactions with the neighboring residues. Next, configurational ensembles of the unperturbed and perturbed states are explored, providing two corresponding sets of low frequency normal modes, $e_\mu^{(0)}$ and $e_\mu^{(P)}$ obtained from the Hessian matrices of energy functions in Eqs. (1) and (2). The allosteric potential, which measures the total elastic work exerted on a residue i due to the change in the displacements of the neighbors (with a distance cutoff $d_c = 11$Å) determined by the normal modes μ is given by

$$U_i(\sigma) = \frac{1}{2} \sum_\mu \varepsilon_{\mu,i} \sigma_\mu^2 \tag{3}$$

with $\varepsilon_{\mu,i} = \sum_{j:d_{ij}^0 < d_c} \left| e_{\mu,i} - e_{\mu,j} \right|^2$, obtained from the corresponding normal modes of both states, and σ is a vector of Gaussian distributed amplitudes, $\sigma = (\sigma_1, ..., \sigma_\mu, ...)$ with variance $1/\varepsilon_{\mu,i}$. The vector σ represents a configurational state of the residue i as the generic displacement of i is $\delta r_i(\sigma) = \sum_\mu \sigma_\mu e_{\mu,i}$.

Subsequently, the allosteric potential evaluated for a residue i in the unperturbed and perturbed states in Eq. (3) is integrated over all possible configurational states σ to obtain the corresponding local partition functions

$$z_i = \int d\sigma e^{-U_i(\sigma)/k_B T} = \prod_\mu \left(\pi \frac{2k_B T}{\varepsilon_{\mu,i}} \right)^{1/2} \tag{4}$$

which allow one to calculate the free energies $g_i = -k_B \ln z_i + constant$, hence, the per-residue free energy change upon a perturbation P is

$$\Delta g_i^{(P)} = \frac{1}{2} k_B T \sum_\mu \frac{\varepsilon_{\mu,i}^{(P)}}{\varepsilon_{\mu,i}^{(0)}}. \tag{5}$$

A positive value of $\Delta g_i^{(P)}$ indicates an increase of configurational work exerted on residue i, which may lead to conformational changes, due to changes in the configurational ensemble of its neighbors upon a

perturbation. In contrast, a negative value of $\Delta g_i^{(P)}$ may prevent conformational changes.

Since a perturbation can generally cause allosteric response of different signs and magnitudes in most distal residues, we consider the background-free allosteric modulation on a residue i by evaluating the deviation of the free energy change from the mean of all residues in the protein chain

$$\Delta h_i^{(P)} = \Delta g_i^{(P)} - \langle \Delta g_i^{(P)} \rangle_{Prot} \qquad (6)$$

which measures the extent at which the allosteric response in the residue i differs from the global effect of the perturbation. Therefore, the allosteric modulation $\Delta h_i^{(P\downarrow)}$ and $\Delta h_i^{(P\uparrow)}$ quantify the purely allosteric effect on residue i caused by destabilizing DOWN (mimicking introduced disorder) and stabilizing UP (mimicking introduced order) perturbation on residue(s) p, respectively. In order to have a generic description of the allosteric signaling from any protein position to a residue on a site of interest, we also defined the notion of modulation range, which is the maximal range of allosteric signal calculated as a difference between UP and DOWN perturbations

$$\Delta h_i^{(P\downarrow\uparrow)} = \Delta h_i^{(P\uparrow)} - \Delta h_i^{(P\downarrow)}. \qquad (7)$$

In considering the allosteric effect at the level of sites, one can calculate the average modulation value for residues i of the site of interest, $\Delta h_{Site}^{(P)} = \left\langle \Delta h_i^{(P)} \right\rangle_{Site}$.

The per-residue resolution of the SBSMMA allows the exhaustive analysis of allosteric signaling by perturbing all single residues and quantifying the allosteric modulation on every residue. The Allosteric Signaling Map (ASM) introduced elsewhere (Guarnera and Berezovsky, 2019; Guarnera and Berezovsky, 2019) contains the complete description of allosteric signaling which can be instrumental in modifying existing regulatory exosites and rational design of new allosteric site. Here, in addition to performing single-residue perturbations, ASMs were also derived on the basis of two- and three-residue segment perturbations. The magnitude of modulation values should be considered in relation to the thermal fluctuation, with values above $k_B T$ indicating significant allosteric effect. Noteworthy, low $\Delta h_i^{(P)}$ caused by a number of individual residues may constitute a large cumulative allosteric response in the affected site/region of the protein.

3. Results

3.1. Operational definition of protein disorder and observables used in the work

In order to characterize order/disorder and transitions between these two states, we use here the following operational definition. We define protein disorder as the absence of rigid elements of the secondary structure, either in native proteins or as a result of destabilizing (DOWN) mutations in the framework of SBSMMA that mimic substitutions of the original amino acids with the smallest ones (Ala-/Gly-like). The rigidifying or introducing order in the protein chain is achieved via stabilizing (UP) mutations into the bulkiest residues (Phe-/Trp-like) in the place of the original ones. With the above operational definition, order-to-disorder transition results in a loss of the chain rigidity, whereas the opposite transition rigidifies the local protein segments.

We quantify the allosteric signaling to every residues i upon perturbations of all single residues in form of the allosteric modulation ranges $\Delta h_i^{(P\downarrow\uparrow)}$, which are used to compose the allosteric signaling maps (ASMs) for the analysed proteins (Guarnera and Berezovsky, 2019; Tan et al., 2019). The allosteric modulation range represents the maximal possible range of the strength of signaling, which is a result of the difference between the effects of stabilizing (UP) and destabilizing (DOWN) mutations (see Materials and Methods). In the SBSMMA (Guarnera and Berezovsky,

2019; Guarnera and Berezovsky, 2019; Guarnera and Berezovsky, 2016), such perturbation effectively stabilizes the neighbourhood of a mutated residue, resulting in modulation ranges (kcal/mol) that are mostly negative ($\Delta h_i^{(P\downarrow\uparrow)} < 0$) from the vicinity of the perturbed residue up to the chain/domain border, but chiefly positive ($\Delta h_i^{(P\downarrow\uparrow)} > 0$) in remote locations and other chains/domains (Guarnera and Berezovsky, 2019; Tan et al., 2019). At the same time, complexity of the protein tertiary/quaternary structures and local peculiarities in their individual chains/domains may result in distinctions in the sign and value of allosteric modulation in some locations of these structural units. In other words, while it is expected to observe that disorder-to-order transition will typically stabilize surrounding residues within the perturbed structural unit and will cause some conformational changes in other parts of the structure, it can also happen that disorder-to-order transition will cause conformational changes on certain residues located in the perturbed chain/domain and, at the same time, will prevent conformational changes in remote parts of the protein. The opposite scenario is expected for the effects of order-to-disorder transition. To this end, our first goal here was to learn how disorder-to-order transition and *vice versa* can be involved in different phenomenologies of the allosteric regulation of protein activity, such as formation of the dimer interface in BirA (Wang et al., 2017), preorganization of the binding pocket in SrtA (Pang and Zhou, 2015), and blocking the active conformation of Rac1 by engineered extrinsic disorder (Dagliyan et al., 2016). Then, using the exhaustive description of allosteric signaling contained in the ASMs of a set of esterase homologues with different thermostability, we addressed a question of a generic strategy for disorder/order-based allosteric tuning of protein activity.

3.2. Disorder-to-order transition in two distant sites in BirA mediated by allosteric communication

The *Escherichia coli* BirA (Fig. 1a) is a bifunctional biotin ligase and a biotin operon repressor (Eisenstein and Beckett, 1999): (i) it catalyzes the transfer of biotinoyl-5′-AMP (bio-5′-AMP) to the biotin carboxyl carrier protein subunit of acetyl CoA carboxylase when biotin is in high demand during rapid growth; (ii) it forms a homodimer with bound bio-5′-AMP for transcriptional repression of the biotin biosynthetic operon. Comparison of crystal structures shows that presumably disordered in apo BirA monomer (not showing electron density, Suppl. Figure S1a), the biotin binding loop (BBL, Arg116—Phe124) and adenylate binding loop (ABL, Met211—Gly222), which bind bio-5′-AMP, and the dimerization interface constituting of two loops (Glu140—Ala146 and Gly193—Ala199), become folded in the holo BirA dimer with two bound bio-5′-AMP molecules (Fig. 1a and Suppl. Figure S1a). Double-mutant cycle analysis together with thermodynamic measurements revealed a coupling between residues in the binding site and dimerization interface, which are separated by approximately 30 Å, suggesting that disorder-to-order transitions in both IDRs are mediated by allosteric communication (Wang et al., 2017).

We derived the Allosteric Signaling Map (ASM, Fig. 1b) of BirA monomer (PDB: 2ewn), which quantifies the allosteric signaling caused by the single-residue perturbations in form of the modulation range $\Delta h_i^{(P\downarrow\uparrow)}$ (see also Materials and Methods). We also obtained the ASMs with signaling caused by exhaustive perturbations of two and three residues in BirA, provided along with distance maps in Suppl. Figure S2a. To understand the allosteric communication between the effector binding site and dimerization interface in BirA (Wang et al., 2017), we quantified the modulation ranges in the interface caused by single-residue perturbations in the effector binding site and compared them with modulation obtained by the perturbation of other positions in the structure (Fig. 1c). The plot shows that the sign of modulation ranges changes from negative to positive at approximately 20 Å, showing the increase in configurational work exerted in the dimerization interface as a result of the perturbation of residues distant from the interface. Strikingly, the plot shows several outliers located between 30 and 40 Å from the interface

that cause negative modulation ranges (Fig. 1c). Among them are residues in the C-terminus and, remarkably, residues 219–222 in the disorder adenylate binding loop (ABL, Fig. 1a, orange) with per-residue $\Delta h_{\text{dimer}}^{(P\downarrow\uparrow)}$ values at −0.58, −0.64, −0.43 and −0.36 kcal/mol, respectively. Disorder-to-order transition in the ABL causes stabilization of the dimer interface (negative modulation ranges marked by orange in Fig. 1c), while the ordering of the BBL (green, Fig. 1a,c) does not cause stabilization in the dimer interface. These observations suggest that interactions between adenosine of bio-5′-AMP and the disorder ABL stabilizes the ABL and the distal dimerization interface via direct interaction and allosteric signaling, respectively. This conclusion agrees with the concerted disorder-to-order transition in both IDRs observed in experiments (Wang et al., 2017).

We further explored and compared the per-residue modulation ranges in the interface caused by perturbing different residue(s) in the ABL. It appears that perturbations of individual residues can originate strong stabilizing effect on the interface residues 193–199 (Fig. 1d). Additionally, residues 219, 220 originate negative modulation on residues 140–144 and 193–199, whereas perturbation of residues 221, 222 as well as combinations that include these positions result in positive modulation on some residues in segments 140–144 and 193–199 (Fig. 1d). Regardless of the number and combination of perturbed residues, the largest negative modulation ranges are consistently observed on residues 194 and 195, and the modulation magnitudes increase with the number of perturbed residues. For example, perturbing residue 219 results in modulation ranges at −0.87 and −0.96 kcal/mol on residues 194 and 195, respectively, whereas $\Delta h_{194}^{(219-221\downarrow\uparrow)} = -1.66$ and $\Delta h_{195}^{(219-221\downarrow\uparrow)} = -1.79$ kcal/mol. The crystal structure of the holo BirA dimer shows that Lys194 and Thr195 in the β-hairpin turn, which are flanked by glycines, interact with the BBL of the dimer partner. It suggests, therefore, that allosteric signaling originated from the ABL (especially, residues 219 and 220) leads to a decrease in the configurational work in residues 194 and 195, which may facilitate folding of the IDR where dimerization occurs. Additional perturbations of residues 221 and 222, at the same time, may be involved in the re-structuring of the allosterically-induced interface via conformational changes.

Fig. 1e illustrates how perturbations of residues 219, 220 can cause large negative allosteric modulation on residues of the dimer interface ($\Delta h_{Dimer}^{(219\downarrow\uparrow)} = -0.58$ and $\Delta h_{Dimer}^{(220\downarrow\uparrow)} = -0.64$ kcal/mol, top panels) in comparison with the effect of perturbations of residues 208 and 223 (used as a negative control), which originate positive modulation from outside of the ABL region ($\Delta h_{Dimer}^{(208\downarrow\uparrow)} = 0.30$ and $\Delta h_{Dimer}^{(223\downarrow\uparrow)} = 0.04$ kcal/mol, middle panels). Perturbing single residues 219 and 220 causes a stabilizing effect well localized in the disordered ABL region (top panels, Fig. 1e), which undergoes disorder-to-order transition upon binding bio-5′-AMP. Increasing the number of perturbed residues for example residues 219–221, however, may over-stabilize the adjacent regions of the protein that are folded (bottom panels).

3.3. Calcium ion binding in the intrinsically disordered region leads to allosteric activation of SrtA

Sortase enzymes of gram-positive bacteria are important virulence factors that recognize and cleave a cell-wall sorting signal (LPXTG) of surface proteins, followed by transpeptidation of the proteins to the cell wall. The catalytic domain (residues 60–206) of *Staphylococcus aureus* sortase A (SrtA) is an important target in developing new antibodies due to their crucial role in the pathogenicity. The SrtA is allosterically activated by Ca^{2+} that binds in the β3/β4 loop and the C-terminal end of the β6/β7 loop (Arg159—Lys177), coordinated by residues Glu105, Glu108 (in the β3/β4 loop) and Glu171. Structural studies of the apo SrtA enzyme (shown in Fig. 2a) indicated that the β6/β7 loop is an intrinsically disordered region with low order parameters in nuclear magnetic resonance (NMR) (Naik et al., 2006) and poorly resolved in X-ray crystallography experiments (Zong

et al., 2004). On the other hand, the holo structure with bound sorting signal and allosteric activator Ca^{2+} shows that β6/β7 loop is docked to the protein domain, and the β7/β8 loop, which forms the lid over the sorting signal, is displaced (Suppl. Figure S1b). These observations, along with computational studies using molecular dynamics simulations (Pang and Zhou, 2015), suggest that folding of the disordered β6/β7 loop upon Ca^{2+} binding leads to conformational changes in the β7/β8 loop via allosteric signaling, which is required for the entry of sorting signal.

Similar to the case study of BirA above, we started from the analysis of the ASMs of apo SrtA (PDB: 1t2p) derived for the single-residue perturbations (Fig. 2b) and upon perturbations of two and three residues (Suppl. Figure S2b). To identify perturbations that could result in the conformational changes of the β7/β8 loop, we analysed the modulation ranges $\Delta h_{\beta7/\beta8}^{(P\downarrow\uparrow)}$ caused by single-residue perturbations in the β6/β7 loop and other parts of the structure (Fig. 2c). The plot of the modulation ranges shows a change in the sign from negative to positive at about 20 Å, marking the distance at which allosteric effects start to dominate over those caused by direct interactions. Perturbation of residues 171–177 (orange, Fig. 2a) in the disordered β6/β7 loop causes positive allosteric modulation $\Delta h_{\beta7/\beta8}^{(P\downarrow\uparrow)}$ in the β7/β8 loop, suggesting that disorder-to-order transition of the β6/β7 loop upon binding Ca^{2+} causes an increase of work exerted on the β7/β8 loop that can initiate conformational changes and facilitate, thus, substrate's entry to the cleavage site.

The $\Delta_{\beta7/\beta8}^{(P\downarrow\uparrow)}$ value generally increases with the number of residues perturbed in the C-terminal end of the β6/β7 loop (Fig. 2d). For example perturbations on residue 177 and residues 175–177 cause per-residue modulation ranges at 2.43 and 4.93 kcal/mol in the β7/β8 loop, respectively. Fig. 2e illustrates more details of the allosteric regulation in SrtA involving disorder-to-order transition. The top row shows that perturbation of residue 177 and residues 176–177 stabilize the C-terminal region of the β6/β7 and β3/β4 loops, which constitute the Ca^{2+} binding site. Interestingly, in addition to the positive modulation range in the distal β7/β8 loop, we also observed an increase of configurational work exerted in the β4/H2 loop (residues 121–131), which was suggested as the binding site for lipid II (Jacobitz et al., 2017) - another substrate in transpeptidation. The observed signaling indicates that Ca^{2+} binding in the IDR likely leads to the conformational changes required for preorganization of the binding pocket for both sorting signal and lipid II via allosteric signaling. Notably, the β3/β4 loop is highly enriched with charged and polar residues from Glu105 to Asp112 (Glu-Glu-Asn-Glu-Ser-Leu-Asp-Asp), which indicates that this region is likely to be disordered as well. We show that perturbing residues 110 and 111 in the β3/β4 loop also causes positive modulation ranges in the lid and the lipid II binding site (Fig. 2e, middle panels), predicting the potential allosteric effect of disorder-to-order transition in the β3/β4 loop. Additionally, a computational study by Pang and Zhou showed that interactions of Ca^{2+} with negatively charged residues in the β3/β4 loop precedes the docking of the C-terminal end of the β6/β7 loop to the protein domain (Pang and Zhou, 2015). We found that perturbing the β3/β4 loop (for example, residues 110 and 111) causes an increase of configurational work in the β6/β7 loop, possibly facilitating its docking to the domain and subsequent stabilization by electrostatic interaction between Glu171 and calcium ion (Fig. 2e, middle panels). At the same time, perturbation of residues 105 and 171 performed as a control experiment did not show any significant allosteric effect in the β7/β8 and β4/H2 loops (Fig. 2e, bottom panels). Taken together, above data show that the functional activity of SrtA can be allosterically regulated by perturbation in the C-terminal end of disordered β3/β4 and β6/β7 loops where Ca^{2+} binds, consistent with the mechanism of allosteric activation by Ca^{2+} binding documented in other experimental and computational studies.

3.4. Extrinsic disorder for allosteric control of Rac1

While allosterically-induced dimerization of BirA and substrate binding in SrtA exemplify the effects of disorder-to-order transition in these
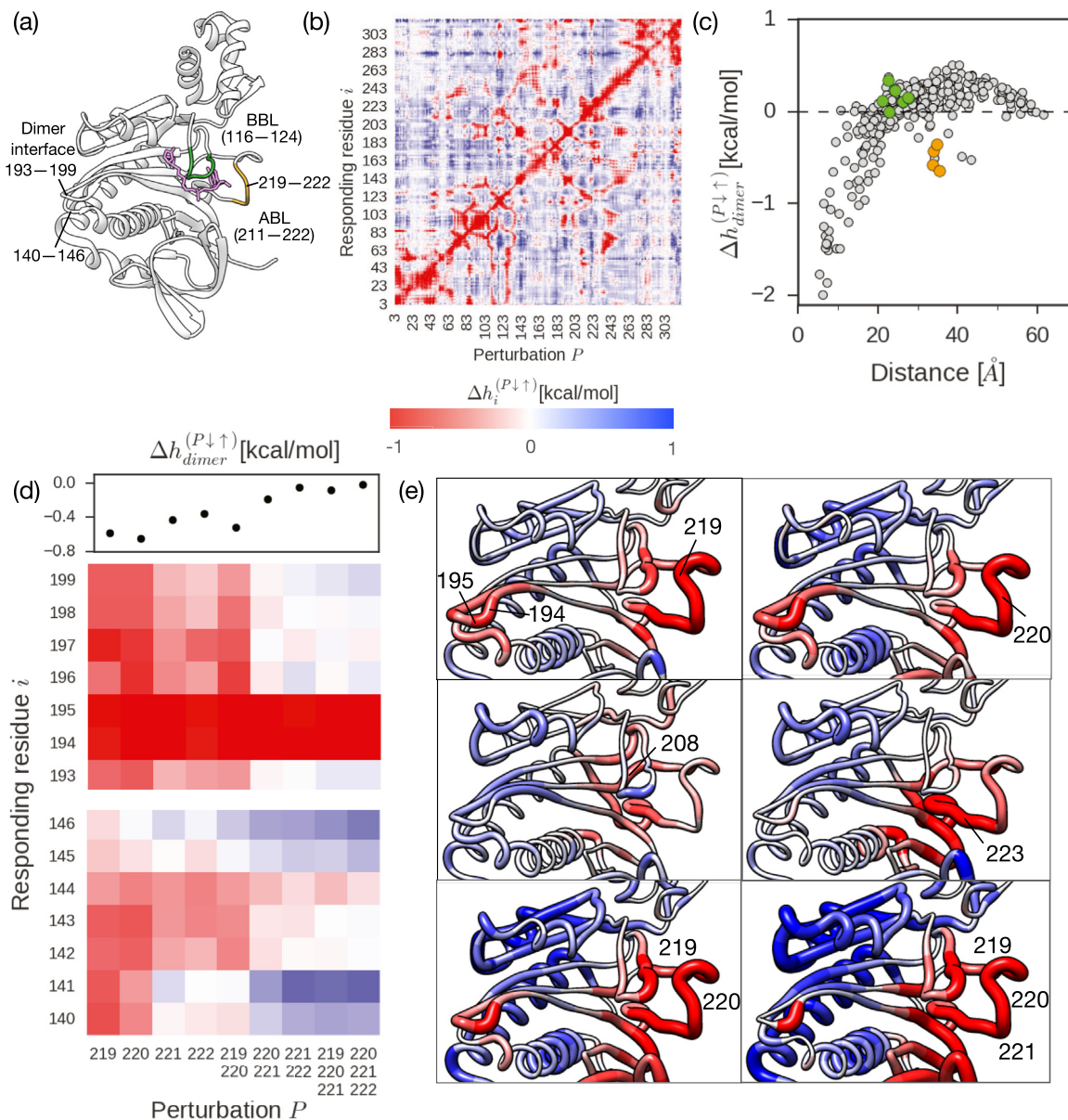
Fig. 1. Allosteric communication mediating disorder-to-order transitions in BirA and its dimerization. (**a**) The crystal structure of BirA monomer (PDB: 2ewn). Dimer interface (residues 140–146 and 193–199) is indicated; the BBL (residues 116–124) is colored in green and residues 219–222 within the ABL (211–222) are colored in orange. Bound bio-5′-AMP is shown in pink. (**b**) The exhaustive Allosteric Signaling Map (ASM), which contains modulation ranges $\Delta h_i^{(P\downarrow\uparrow)}$ (kcal/mol) exerted at residue i due to perturbation at residue P. The red-to-blue color gradient is used to indicate negative-to-positive range of $\Delta h_i^{(P\downarrow\uparrow)}$ values. (**c**) Scatter plot of modulation ranges in the dimer interface $\Delta h_{dimer}^{(P\downarrow\uparrow)}$ upon disorder-to-order transition at residue P versus the average distance between the perturbed residue and residues constituting the interface. The $\Delta h_{dimer}^{(P\downarrow\uparrow)}$ values due to residues in the BBL and residues 219–222 in the ABL are indicated in green and orange, respectively. (**d**) The $\Delta h_{dimer}^{(P\downarrow\uparrow)}$ caused by perturbing single, two and three residues in the ABL (upper panel) and the per-residue modulation values in the interface from the ASMs (lower panel). (**e**) The structure of BirA colored according to the modulation ranges caused by disorder-to-order transition of residues located in the ABL. The perturbed residues (219–222) and residues 208 and 223 as negative controls are labelled. The color scheme follows that in (b) and the radius of the tube-like depiction represents the magnitude of the modulation.

proteins, exogenous domains, such as the LOV2 domain, have been artificially engineered into multiple proteins to introduce extrinsic disorder at the insertion site. Here, we show that the SBSMMA describes the causality of light-induced order-to-disorder transition in the allosteric regulation of the guanosine triphosphate phosphohydrolase (GTPase) activity.

The Ras-related C3 botulinum toxin substrate 1 (Rac1), which belongs to the Rho family of GTPases regulates diverse cellular signaling pathways such as cell migration and invasion (Bosco et al., 2009). Rac1 is stimulated by guanine nucleotide exchange factors (GEFs) to exchange GDP for GTP through conformational changes in the Switch 1 (S1, residues 35–39) and
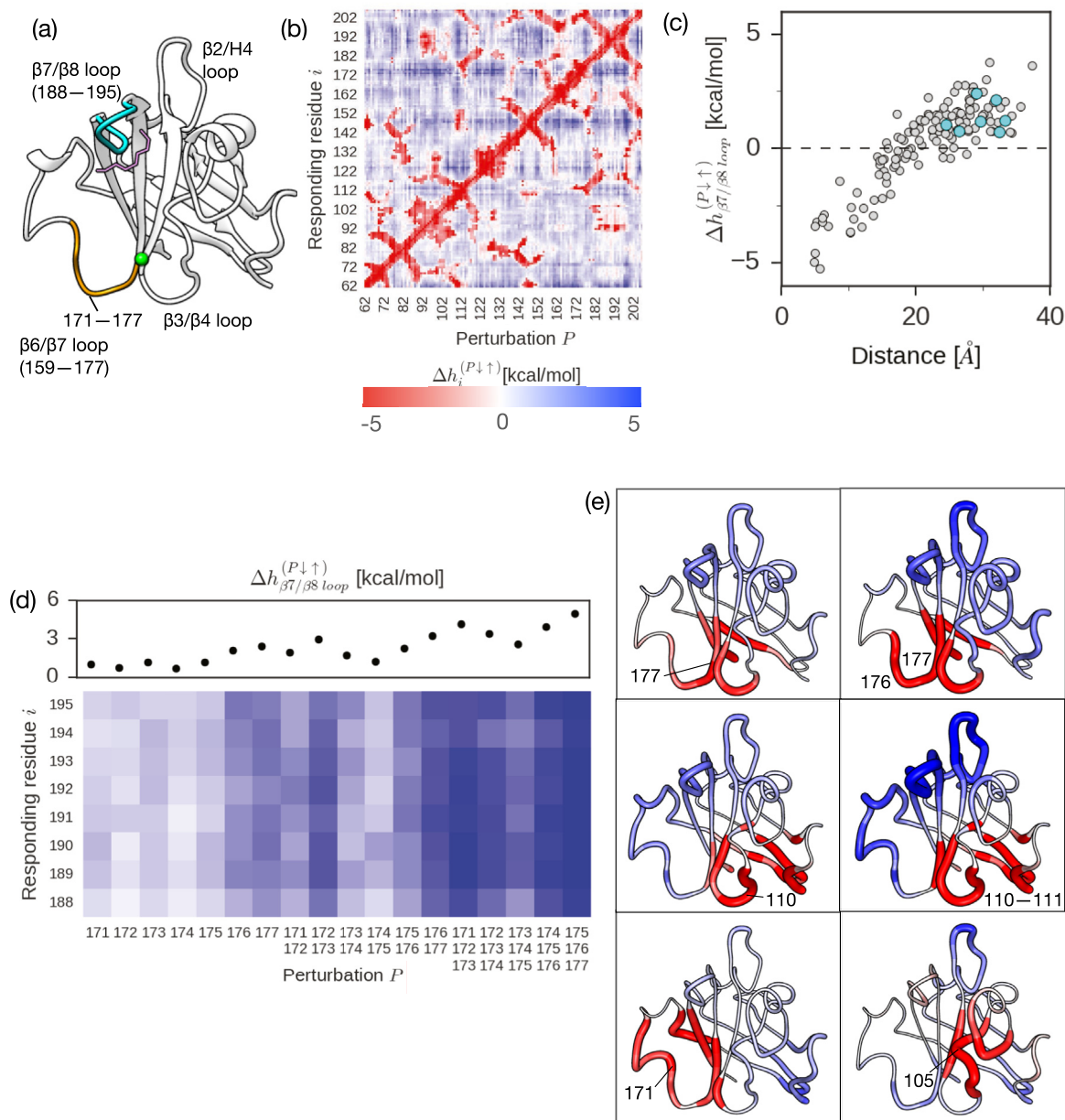
Fig. 2. Allosteric signaling caused by calcium ion binding to the IDR in SrtA. (**a**) The crystal structure of apo SrtA (PDB: 1t2p). Calcium ion (green) and sorting signal (pink) are superimposed on the apo structure for illustration. Residues 171–177 in the β6/β7 loop are colored in orange and the β7/β8 loop is colored in cyan. (**b**) The ASM derived for SrtA. (**c**) The $\Delta h^{(P\downarrow\uparrow)}_{\beta7/\beta8\ loop}$ values upon disorder-to-order transition at perturbed residue P plotted against the average distance between residue P and residues in the β7/β8 loop. Modulation ranges caused by perturbing residues 171–177 in the β6/β7 loop are colored in cyan (**d**) The $\Delta h^{(P\downarrow\uparrow)}_{\beta7/\beta8\ loop}$ caused by perturbing single, two and three residues from 171 to 177 (upper panel) and the per-residue modulation values in the β7/β8 loop from the ASMs (lower panel). (**e**) The structure of SrtA colored according to the modulation ranges caused by disorder-to-order transition of the labelled residues. The residues 171 and 105 serve as the negative control.

Switch 2 (S2, residues 57–67) regions of the G domain (Fig. 3a). The active GTP-bound Rac1 then interacts with downstream effector proteins in a multitude of signal transduction pathways. Dagliyan and colleagues have engineered light-sensitive molecular switches into the strategic location at the L1 β-hairpin turn of two anti-parallel β strands, connecting both S1 and S2 in the G domain of Rac1, RhoA, and Cdc42 in the Rho family of GTPases

to achieve robust and reversible control of their *in vivo* functions by light (Dagliyan et al., 2016). Light-induced disordering of the terminal helices of the inserted LOV2 domain (see Fig. 2c in (Dagliyan et al., 2016)) introduces flexibility at the L1 β-hairpin turn, resulting in the allosteric inhibition of the GTPase activity and in the alteration of the morphodynamics of living cells.
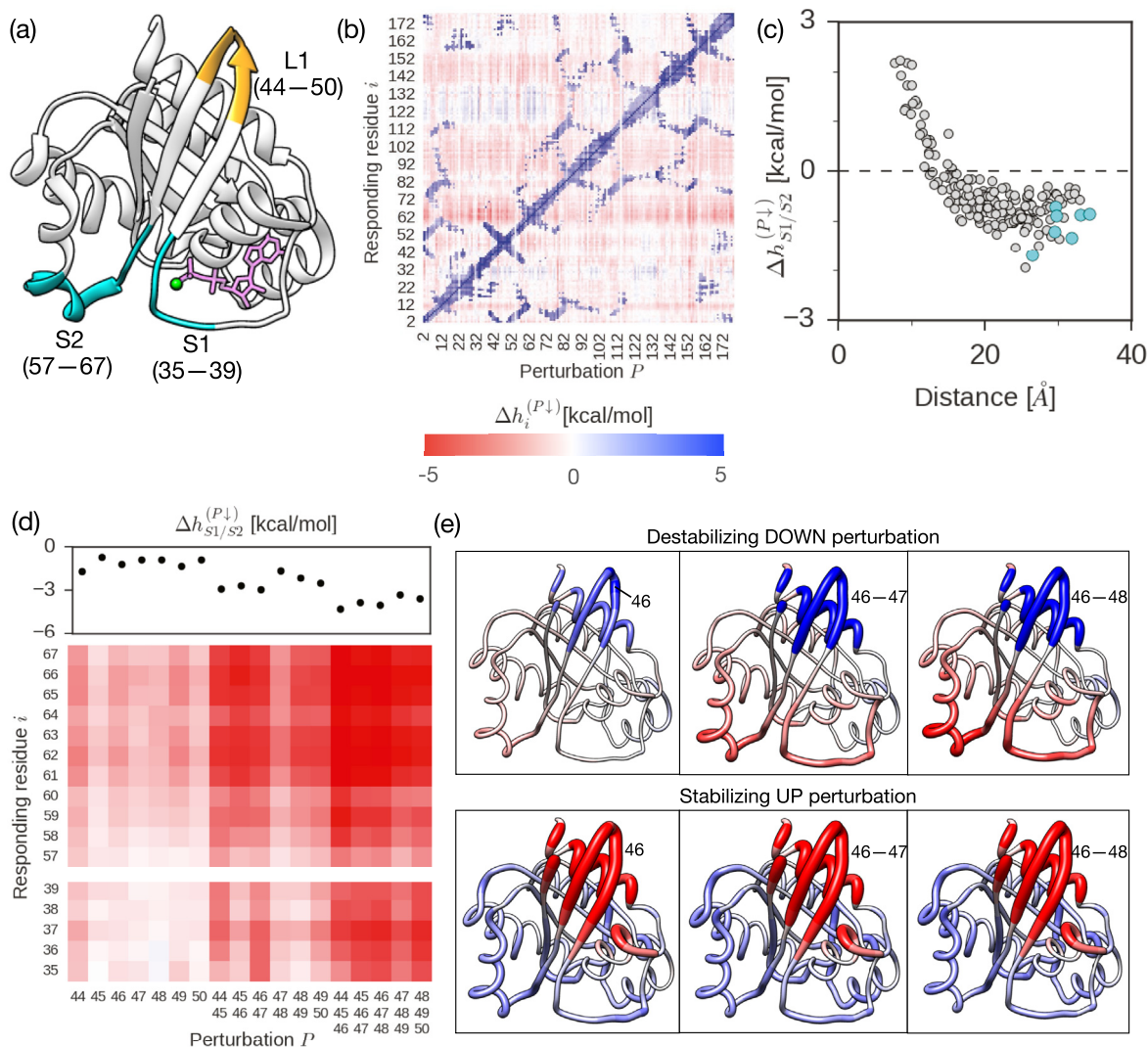
Fig. 3. Allosteric signaling originated by local disorder in Rac1. (**a**) The crystal structure of the inactive Rac1 (PDB: 1i4d). GDP molecule and magnesium ion are colored in pink and green, respectively. L1 (44–50) is colored in orange, S1 (35–39) and S2 (57–67) are colored in cyan. (**b**) The ASM derived for Rac1. (**c**) The $\Delta h^{(P\downarrow)}_{S1/S2}$ values upon simulated disorder at residue P plotted against the average distance between perturbed residue P and residues in the S1 and S2 regions. The modulation values caused by perturbing residues 44–50 in the L1 site are colored in cyan. (**d**) The $\Delta h^{(P\downarrow)}_{S1/S2}$ caused by perturbing single, two and three residues from 44 to 50 (upper panel), and the per-residue modulation values in the S1 and S2 regions from the ASMs (lower panel). (**e**) The structure of Rac1 colored according to the allosteric modulation caused by local disorder (above) and by rigid packing (below) at the labelled residues.

Fig. 3b shows the ASM of the inactive Rac1 (PDB: 1i4d) with the complete information on the allosteric signaling caused by the DOWN perturbations of single residues that mimic local disorder (Fig. 3b). The ASMs derived from perturbing two and three residues and the distance maps are shown in Suppl. Figure S2c. The ASM revealed that single-residue DOWN perturbations in the G domain of GTPase (177 residues) introduce structural disorder in the protein, which destabilizes residues close to the perturbed location and, at the same time, originate allosteric signaling that causes stabilization of distant residues. In order to analyze allosteric modulation on the S1/S2 switches, we plotted the $\Delta h^{(P\downarrow)}_{S1/S2}$ values to investigate the allosteric effect in the S1/S2 region caused by structural disorder at various residual positions of Rac1 (Fig. 3c), especially the signaling from the L1 β-hairpin turn (residues 44–50, Fig. 3a). The plot in Fig. 3c shows that structural disorder near the S1/S2 region causes positive modulation, indicating destabilization and potential conformational changes in the region. The sign of modulation values

changes from positive to negative upon perturbations of increasingly distant positions, demonstrating that order-to-disorder transition at distal locations can stabilize the S1/S2 region. Therefore, in the case of the inactive Rac1, extrinsic disorder at the LOV2 insertion site (orange) can potentially prevent conformational changes in the S1/S2 region (large negative per-residue $\Delta^{(P\downarrow)}_{S1/S2}$ values in Fig. 3c) that are required for interaction with GEFs and GDP release, thereby suggesting a mechanism for the light-induced allosteric inhibition of the Rac1 activity. The ASM shows that disorder in residues 44–50 leads to negative modulation in all residues in the S1/S2 region (Fig. 3d). Moreover, the allosteric modulation on S1/S2 can be enhanced by perturbing more residues in the L1 site, for example, $\Delta h^{(46\downarrow)}_{S1/S2} = -1.20$ and $\Delta^{(46-48\downarrow)}_{S1/S2} = -4.00$ kcal/mol. We also show that while destabilizing DOWN perturbation can emanate a strong allosteric signal specifically to S1/S2 region (Fig. 3e, upper panels), stabilizing UP perturbation in the same positions causes an opposite
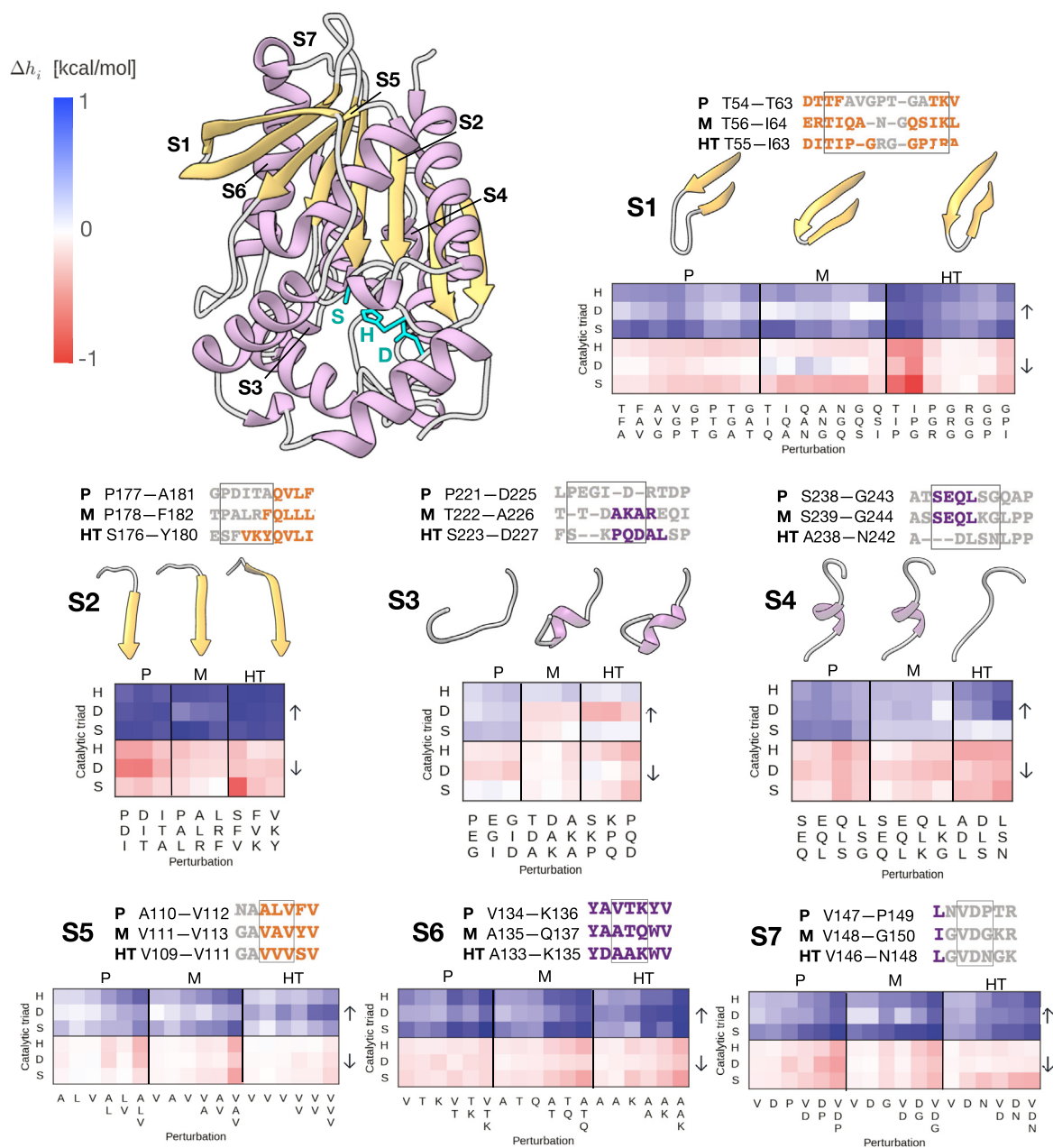
Fig. 4. Inducing allosteric response by tuning structural order and disorder in esterases. On the left, the structure of Est-M (PDB: 4ob8) is shown with the catalytic triad colored in cyan. Segments of protein primary structure that exhibit different (S1–S4) and same secondary structure contents (S5–S7) among the homologues are indicated. On the right and below, sequence alignments of the homologues are shown with the secondary structures colored for each segment, β strand—orange, α helix—purple and loop—grey. Psychrophilic, mesophilic and hyperthermophilic esterases are indicated by P, M and HT, respectively. Single and stretches of two and three residues are perturbed via a sliding window approach within the enclosing black frame. Structures corresponding to the aligned sequences are shown for each segment. The heat maps consist of the per-residue allosteric modulation at catalytic residues (S—serine, D—aspartic acid and H—histidine) due to UP perturbation (above, up arrow) and DOWN perturbation (below, down arrow) are obtained from the ASMs.

allosteric response, albeit less specific one with a mild increase of configurational work exerted in most parts of the protein (Fig. 3e, bottom panels). One can conclude, therefore, that disorder (order)-to-order (disorder) transitions at positions 44–50 can act as an allosteric effector originating different modes of modulation in the functional site and allowing to establish allosteric control of the Rac1 activity.

3.5. Inducing and tuning of allosteric effects via transitions between order and disorder

The regulatory potential of intrinsic disorder observed in BirA (Fig. 1) and SrtA (Fig. 2) and of the extrinsic disordered region in Rac1 (Fig. 3) involving allosteric mechanisms hints at the possibility to use back and
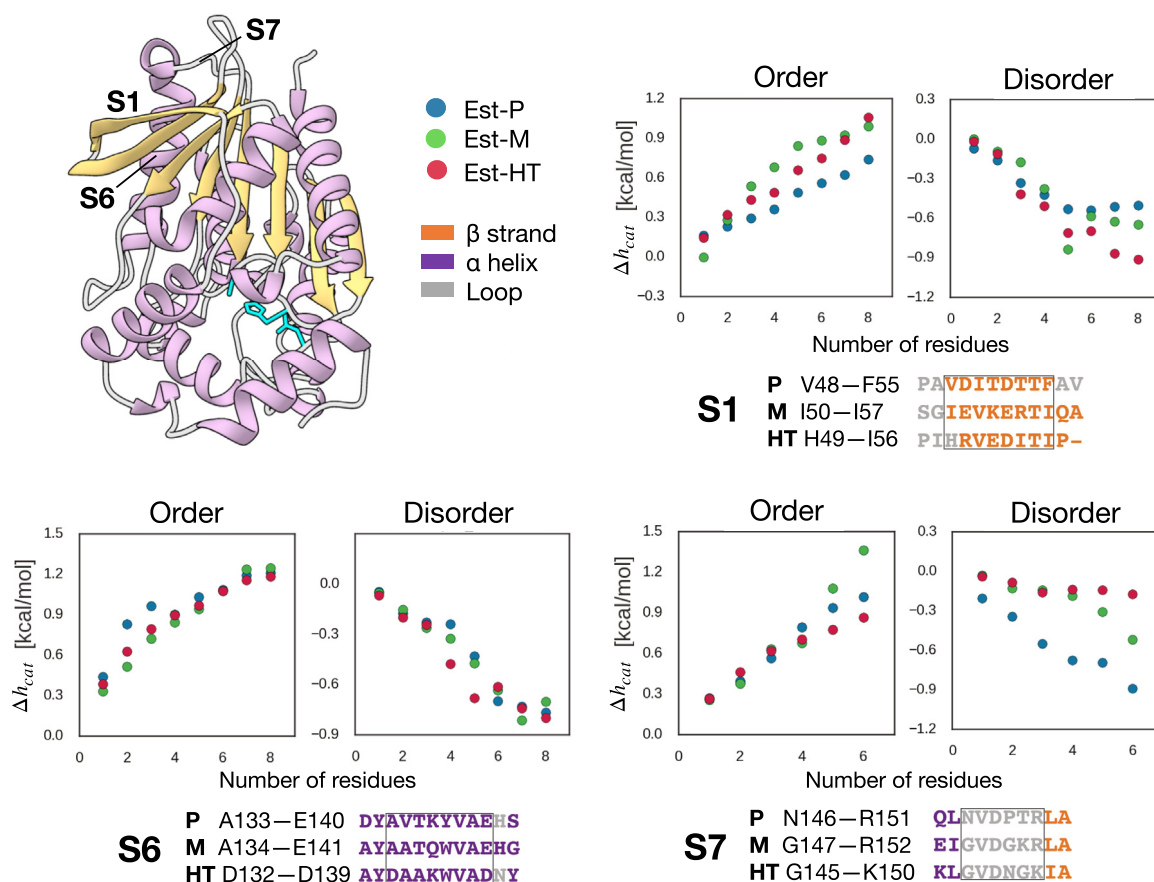
Fig. 5. Incremental tuning of structural order and disorder. Segments S1, S6 and S7 are incrementally perturbed from single to six or eight residues.

forth transitions between order and disorder for inducing allosteric signaling of opposite modes. In order to explore this possibility, we performed corresponding computational experiments on a set of esterase enzymes. While allosteric regulation in these esterases have not been documented, we aim to demonstrate in simulations on the basis of SBSMMA that allosteric signaling can be originated by introducing structural order or disorder in different parts of the protein. The esterases are hydrolases that are extensively used as biocatalysts in various industrial and biotechnological processes for splitting the ester bonds in diverse substrates. The enzyme consists of two subdomains, the bigger subdomain features an α/β-hydrolase fold with 8 central β-strands connected by α-helices, the smaller one consists of α-helices where the substrate binding site is located. The canonical catalytic triad composed of serine, histidine and aspartic acid is situated between the subdomains. Here, we performed exhaustive UP and DOWN perturbations of the esterase (Est) monomer from the marine psychrophilic bacterium *Thalassospira* sp. GB04J01 (Est-P, PDB: 4v2i), the mesophilic *Pseudomonas putida* (Est-M, PDB: 4ob8) and the hyperthermophilic archeon *Pyrobaculum calidifontis* VA1 (Est-HT, PDB: 3zwq). Supplementary Figure S3 contains ASMs obtained for these proteins upon single-/two-/three-residue perturbations and the distance maps. The structures of Est homologs are largely similar with an overall RMSD equal to 1.2 Å (Suppl. Figure S4), allowing to identify a number of segments that exhibit different secondary structure contents on the basis of the structure-based multiple sequence alignment (sequence identity at 26%, Suppl. Figure S5). To make sure that only allosteric signaling to the catalytic

triad is considered, we set the Cα—Cα distance cut off between residues in the segments and the catalytic triad at 17 Å as a criterion in the definition of allosteric interaction.

Our goal here is two-fold: first, we would like to find out how sequence and structural changes in the non-conserved parts of the structural homologues, which is a result of the adaptation to different environmental temperatures, are manifested in the potential changes of allosteric signaling; second, we will explore if allosteric signaling can be induced and altered by disorder/order-to-order/disorder modifications at different parts of the proteins including conserved elements of the secondary structure.

We delineated several segments of residues, S1–S7, from the structure-based multiple sequence alignment of the homologues (Suppl. Figure S5). First, we explored if there are common trends in changing of allosteric effects because of the structural variations associated with thermal adaptation. We considered four segments S1–S4 of the fold with high sequence/structure variability and different elements of secondary structure: segments 1 and 2 (S1 and S2) include β-strands, S3 and S4—α-helices (Fig. 4). Both α and β elements are different in sizes in corresponding segments. For each segment, allosteric modulations at the catalytic residues due to UP and DOWN perturbations in all overlapping windows of three residues are evaluated. In general, increasing of the structural order causes an increase of configurational work that may lead to conformational changes at the distant catalytic triad. Local disorder leads to the opposite effect, which prevents conformational changes. In the structure from hyperthermophilic *P. calidifontis* VA1 (Est-HT), which

is presumably more stable than its psychrophilic (Est-P) and mesophilic (Est-M) homologues, the effects of both increasing order (UP mutations) and increasing disorder (DOWN) are more pronounced. The induced allosteric response can vary depending on the presence or absence of the secondary structure elements in proteins from different organisms (Fig. 4). For example, Segment 3 (S3) of Est-HT contains an α–helical piece that reduces the allosteric effects on the catalytic triad upon mutations (both UP/ordering and DOWN/disordering) in S3, whereas ordering of the unstructured loop in S3 of Est-P provides a potential for conformational changes in the active site of the esterase (Fig. 4). At the same time, increasing order/disorder in the flexible loop of Est-HT in S4 can induce relatively strong allosteric modulation on the catalytic site, whereas allosteric signaling is relatively weak upon modifications on the α–helical segment in Est-P and even weaker in Est-M.

Switching our attention from the variable to conserved segments in these homologous esterases, we asked a question whether there are persistent trends in the allosteric effects of back and forth disorder-order transitions independent of the local secondary structure of the conserved segments under perturbation. It appears that regardless of the local structural type, enhancing of rigidity in segments of all types (α, β, and loops) is likely to elicit conformational changes at the distal catalytic triad, whereas increased flexibility at the same locations prevents conformational changes (S5–S7, Fig. 4). In most of the cases, the modulation values differ mildly when neighbouring individual residues in the segments are perturbed and between corresponding positions from different homologues. Also, the strength of the induced response increases from perturbations of single to three residues. To corroborate an apparently generic possibility of using order/disorder for allosteric modulation of protein activity, we further explored a potential of allosteric tuning upon perturbation of longer segments of the protein chain. Extending structural order and disorder up to eight residues within the β-strand near S1, in the α-helix of S6, and up to six residues in the S7 loop (Fig. 5), we show that the magnitude of per-residue allosteric modulation on the catalytic triad Δh_{cat} increases as more residues are perturbed. Fig. 5 also shows that in the case of esterases, ordering of the segment of flexible loops (via stabilizing UP mutations of several consecutive residues) results in a stronger allosteric modulation than upon modifications of residues in β-strands and α-helices. Introducing disorder makes rather similar modulations regardless of the secondary structure type or its absence in the mutated protein residues (Fig. 5). Taken together, the observations summarized in Fig. 5 show that perturbations introducing rigidity or flexibility on distal residues can lead to opposite allosteric modulation on the catalytic site, the strength of which can be fine-tuned on a residue-by-residue basis.

4. Discussion

Studies of protein allostery, started more than 60 years ago from simple phenomenological models to recent elucidation of allosteric mechanisms in various proteins furnished with atomistic details, have produced invaluable understanding of how Nature harness allostery to regulate a spectrum of protein activities (Guarnera and Berezovsky, 2016; Gunasekaran et al., 2004; Tsai & Nussinov, 2014). Since the last decade, the quest on utilising allostery for non-competitive remote modulation of protein functions has yielded many promising outcomes (Guarnera et al., 2017), most notably in developing allosteric drugs (Berezovsky, 2013) and in understanding and using allosteric effects of mutations (Tee et al., 2019). More recently, the allosteric effects of disorder-to-order transition in intrinsically disordered regions (IDRs) have been observed and investigated in a number of proteins (Ferreon et al., 2013; Wang et al., 2017; Pang and Zhou, 2015; Sevcsik et al., 2011). For instance, theoretical work by Hilser and colleagues considers multi-domain proteins as composed of discrete unstructured and structured domains with low and high ligand affinities, respectively (Hilser and Thompson, 2007; Li et al., 2017; Motlagh et al., 2014).

Perturbations, such as disorder-to-order transition as a result of the effector binding would lead to alterations in the energy landscape with a population shift towards states with certain levels of activity. Experimentally, nitration of tyrosine residues in the intrinsically disordered C-terminal domain of the protein α-synuclein, which increases the bulkiness of these residues, was found to allosterically modulate the membrane binding affinity of the distal N-terminal domain (Sevcsik et al., 2011). Recognizing the emerging potential of allosteric modulation originated from the alteration of structural order and disorder, extrinsic perturbations, such as destabilizing mutations and sensory domains, have also been engineered in proteins (Li et al., 2017; Karginov et al., 2010; Dagliyan et al., 2016; Saavedra et al., 2018). For example, entropy-enhancing mutation of alanine to glycine in the AMP binding domain of the adenylate kinase from *E. coli* was found to allosterically affect the catalytic CORE domain which, in turn, regulates the enzyme turnover (Saavedra et al., 2018).

All the above shaped the goal of this work, which is aimed at developing the computational framework and establishing the set of general rules for using disorder/order and transitions between them in allosteric regulation of the protein function. We started from demonstrating the capability of the structure-based statistical mechanical model of allostery (SBSMMA) to describe previously characterized allosteric mechanisms underlying BirA dimerization (Wang et al., 2017), SrtA activation (Pang and Zhou, 2015), and Rac1 inhibition (Dagliyan et al., 2016), which involve order-disorder transitions. To our knowledge, the SBSMMA used here is the first structure-based model, which allows one to account for the causality of disorder-mediated allostery upon simulating order (disorder)-to-disorder (order) on the level of single residues. We showed that alteration of order/disorder upon binding of allosteric activator in BirA and SrtA, and the light-induced extrinsic disorder at the LOV2 insertion site in Rac1 originate specific allosteric signaling to the regulated functional sites with large magnitudes of allosteric modulation (Panels c and e in Figs. 1–3). The allosteric effects quantified by the SBSMMA, in terms of stabilization or destabilization, are consistent with the experimental studies (Dagliyan et al., 2016; Wang et al., 2017; Pang and Zhou, 2015) on the disorder-driven allosteric regulation in these proteins. Specifically, we showed how disorder-to-order transition upon binding of bio-5′-AMP in the disordered loop in BirA may facilitate BirA dimerization, by originating allosteric signaling that results in stabilization of the dimer interface at about 30 Å away. While most of the distal perturbations located more than 20 Å from the dimerization interface cause positive allosteric modulation, ordering of residues 219–222 in the intrinsically disordered adenylate binding loop (ABL, orange) stabilizes the interface (Fig. 1c), consistent with the experimental observation on the concerted disorder-to-order transitions in BirA (Wang et al., 2017). Notably, this allosteric signaling is specific up to per-residue resolution—perturbing single residues 219 and 220 in the ABL causes strong allosteric response at residues 194 and 195 in dimerization interface, whereas perturbing residues 208 and 223 adjacent to the ABL (negative control) does not elicit the allosteric response (Fig. 1e). In SrtA, binding of the allosteric activator Ca^{2+} to the C-terminal regions of disordered β3/β4 and β6/β7 loops increases the configurational work exerted at the distal β7/β8 loop and lipid II binding site that may induce conformational changes, allowing the entry of substrates to the active site. The increase in the configurational work exerted to the ligand entry sites upon Ca^{2+}-induced folding of the disordered β3/β4 and β6/β7 loops is in a good agreement with the conformational changes from the apo to the holo states of the SrtA (Suppl. Figure S1b), especially at the β7/β8 loop forming a lid over the catalytic site. Simulating local disorder at the LOV2 insertion site in the inactive Rac1 prevents conformational changes in the Switch 1 and 2 regions, which are required for the exchange of GDP to GTP. Remarkably, perturbing residues in the insertion site causes the strongest modulation in the S1/S2 regions, with the disorder-driven allosteric stabilization localized within the regions only, in agreement with the observation that conformational changes induced by the light-controlled extrinsic disorder at L1 are manifested chiefly in the S1/S2 regions
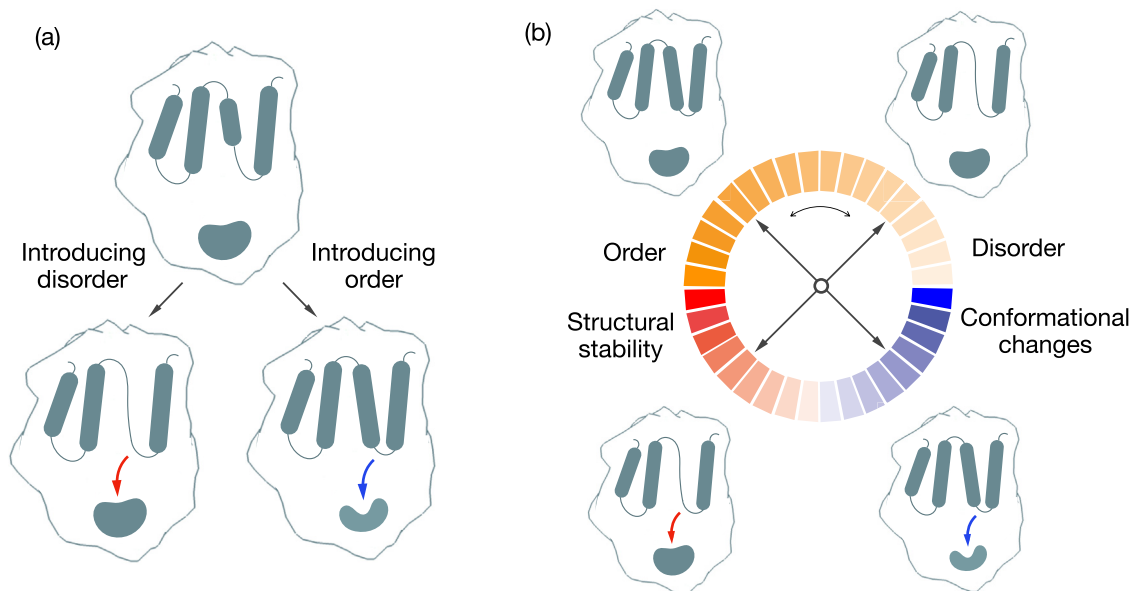
Fig. 6. Disorder-order transitions establish the allosteric control scale of protein activity. (**a**) Introducing structural order and disorder at distal locations leads to the inducing and preventing the conformational changes at protein functional site, respectively. Red and blue arrows indicate a decrease and increase of configurational work exerted at the site. (**b**) The allosteric control scale can be used as a gauge for measuring and tuning the allosteric response on the basis of the extent of disorder/order-order/disorder transitions.

(Dagliyan et al., 2016). Our results also suggest that engineered structures with different order/disorder characteristics at the L1 site can lead to opposite allosteric effects by causing and preventing conformational changes, respectively, in the distal Switch 1 and 2 regions.

Altogether, above case studies show that the SBSMMA (Guarnera and Berezovsky, 2019; Guarnera and Berezovsky, 2019; Guarnera and Berezovsky, 2016) provides an adequate quantitative description of the allosteric regulation governed by structural disorder/order and transitions between them. Therefore, we decided to explore a possibility of using disorder-order relationship in the allosteric tuning of protein activity, using esterases from psychrophilic (*Thalassospira* sp. GB04J01), mesophilic (*P. putida*) and hyperthermophilc (*P. calidifontis* VA1) prokaryotes as model proteins. Analysing these homologs, we found that in addition to variations in the secondary structure elements associated with structure-based strategy of thermal adaptation (Berezovsky and Shakhnovich, 2005; Berezovsky et al., 1997), they can also be involved in the tuning of the allosteric signaling in corresponding proteins. Noteworthy, inclusion/exclusion of secondary structure elements can be used discretely in proteins from organisms adapted to different environmental temperatures. For example, distinctive presence of α-helical elements in S3 of Est-M and Est-HT, and S4 of Est-P and Est-M leads to tuning of the allosteric signal at the catalytic triad, presumably modulating the enzymes' activity and its regulation under different environmental conditions.

In addition to the specifics in potential allosteric tuning in homologs from organisms adapted to extreme environmental temperatures, we observed persistent trends that are present in conserved parts of all esterases regardless of the secondary structure type or its absence. Specifically, we found that introducing structural order in any conserved segment of the structure leads to allosteric modulation of protein activity in the form of inducing conformational changes in the regulated site (Figs. 5 and 6a). Introducing disorder, on the contrary, prevents structural changes in the distal regulated site, and the strength of the modulation gradually increases with the number of perturbed residues (Figs. 5 and 6a). We also found that there is an apparent dependence of the level of allosteric modulation on the type of the secondary structure that was perturbed and on the type of the

perturbation: introducing structural order in flexible loops causes a more pronounced allosteric effect, whereas disorder introduced in β-strands, α-helices, and loops leads to allosteric modulation of similar strength. The Allosteric Signaling Maps (ASMs) also show that stronger allosteric response can be elicited by simultaneously perturbing multiple residues in all the proteins studied here. The ASMs obtained from two/three-residue perturbations in BirA, SrtA and Rac1 are shown in Suppl. Figure 2, and those from the esterases are shown in Suppl. Figure 3. While these observations may suggest potential allosteric effects corresponding to variations in the extents of rigid/flexible structural elements from homologous proteins (in addition to their involvement in protein stability), they also point to the possibility of tuning the desired allosteric responses via extrinsic alterations of order/disorder of varying magnitudes (Fig. 5).

In general, allosteric effects induced by engineered disorder/order or by other perturbations can be predicted and interpreted if the information about the allosteric effect of natural allosteric effector(s), such as ligand binding and/or disorder-order transitions, is available. In this case, the mode of signaling (activating or inhibiting) and its strength can be estimated on the basis of the comparison with those of natural allosteric effectors. The ASMs can be used as a guide to explore protein sites/regions that can lead to or prevent conformational changes in a targeted site, for example the active site of the esterases, and to estimate the energetics of the signaling, upon altering the order/disorder characteristics of the perturbed sites/regions. In the absence of any experimental data on the function-related protein energetics and on the role of allosteric effectors, the predictive potential of our model includes localization of allosteric sites and the strength of the signaling, as it was described elsewhere (Tee et al., 2018; Tan et al., 2020). Noteworthy, both negative and positive modulations can be either activating or inhibiting to the protein function. For example, positive modulation on the active site can either disrupt the interactions between the substrate and the catalytic residues, or facilitate substrate binding, resulting in allosteric inhibition or activation, respectively. At the same time, negative modulation can either hinder the enzymatic activity due to a rigidified active site, or increase the protein activity by stabilizing flexible loops constituting the

active site. In this work, negative allosteric modulation (stabilization) at the disordered dimer interface of the BirA monomer facilitates formation of the active BirA dimer. On the other hand, negative modulation prevents the conformational changes in the Switch regions that are required for Rac1 activation.

The allosteric tuning of protein activity by structural order/disorder, and the potential for its engineering guided by the ASMs were explored here on three case studies and on a set of homologous esterases. On the basis of the observed persistent trends, a generic approach on using introduced disorder or order is proposed for inducing allosteric modulation of protein activity, and for design of proteins with allosteric mechanisms (Tee et al., 2019). Briefly, using the SBSMMA, one can begin by exploring the type of perturbations (either disorder-to-order transition or *vice versa*) that can potentially cause the required mode of allosteric regulation (activation or inhibition) over the protein activity. Next, establishing the quantitative relationship between the degree of introduced order/disorder and the corresponding allosteric effects on the protein function will help to delineate the extents of required modifications/perturbations for inducing the targeted allosteric responses of variable strength. The observed correspondence of the strength of allosteric modulation with the extents of order-disorder transitions (natural or engineered) in the proteins (Figs. 4 and 5) allows to establish the allosteric control scale that can facilitate protein engineering efforts (Fig. 6b). The allosteric control scale can be used as a gauge for estimating the effect of the back-and-forth gradual transition in the order-disorder continuum on the activity of regulated functional sites, via stimulating/preventing conformational changes and modulating their dynamics. Obviously, the structural dependence of allosteric modulation should be further studied on a big number of diverse protein folds, which will also contribute to the multisided picture of the allosteric regulation.

Concluding this work, we argue that order/disorder widely used in natural proteins as one of the efficient ways of controlling the protein activity via allosteric mechanisms can be used in protein design/engineering efforts. To this end, the allosteric control scale can be used as a foundation for quantifying the ground-level allosteric effects of the order/disorder, to be further complemented upon consideration of proteins' structural and functional diversity.

Credit authorship contribution statement

Wei-Ven Tee: performed the work, analyzed data, wrote and edited paper. **Enrico Guarnera:** analyzed data and edited paper. **Igor N. Berezovsky:** supervised the work, wrote and edited paper.

Declaration of competing interest

The authors declare that they have no known competing financial interests or personal relationships that could have appeared to influence the work reported in this paper.

Acknowledgments

Appendix A. Supplementary data

Supplementary data to this article can be found online at https://doi.org/10.1016/j.crstbi.2020.09.001.

References

Berlow, R.B., Dyson, H.J., Wright, P.E., 2018. Expanding the paradigm: intrinsically disordered proteins and allosteric regulation. J. Mol. Biol. 430, 2309–2320.

Bosco, E.E., Mulloy, J.C., Zheng, Y., 2009. Rac1 GTPase: a "Rac" of all trades. Cell. Mol. Life Sci. 66, 370–374.

Cooper, A., Dryden, D.T., 1984. Allostery without conformational change. A plausible model. Eur. Biophys. J. 11, 103–109.

Dagliyan, O., Tarnawski, M., Chu, P.H., Shirvanyants, D., Schlichting, I., Dokholyan, N.V., Hahn, K.M., 2016. Engineering extrinsic disorder to control protein activity in living cells. Science 354, 1441–1444.

Dunker, A.K., Silman, I., Uversky, V.N., Sussman, J.L., 2008. Function and structure of inherently disordered proteins. Curr. Opin. Struct. Biol. 18, 756–764.

Dunker, A.K., Babu, M.M., Barbar, E., Blackledge, M., Bondos, S.E., Dosztanyi, Z., Dyson, H.J., Forman-Kay, J., Fuxreiter, M., Gsponer, J., et al., 2013. What's in a name? Why these proteins are intrinsically disordered: why these proteins are intrinsically disordered. Intrinsically Disord. Proteins 1, e24157.

Eisenstein, E., Beckett, D., 1999. Dimerization of the Escherichia coli biotin repressor: corepressor function in protein assembly. Biochemistry 38, 13077–13084.

Berezovsky, I.N., Shakhnovich, E.I., 2005. Physics and evolution of thermophilic adaptation. Proc. Natl. Acad. Sci. U. S. A 102, 12742–12747.

Ferreon, A.C., Ferreon, J.C., Wright, P.E., Deniz, A.A., 2013. Modulation of allostery by protein intrinsic disorder. Nature 498, 390–394.

Garcia-Pino, A., Balasubramanian, S., Wyns, L., Gazit, E., De Greve, H., Magnuson, R.D., Charlier, D., van Nuland, N.A., Loris, R., 2010. Allostery and intrinsic disorder mediate transcription regulation by conditional cooperativity. Cell 142, 101–111.

Gsponer, J., Babu, M.M., 2009. The rules of disorder or why disorder rules. Prog. Biophys. Mol. Biol. 99, 94–103.

Guarnera, E., Berezovsky, I.N., 2016. Allosteric sites: remote control in regulation of protein activity. Curr. Opin. Struct. Biol. 37, 1–8.

Guarnera, E., Berezovsky, I.N., 2016. Structure-based statistical mechanical model accounts for the causality and energetics of allosteric communication. PLoS Comput. Biol. 12, e1004678.

Guarnera, E., Berezovsky, I.N., 2019. On the perturbation nature of allostery: sites, mutations, and signal modulation. Curr. Opin. Struct. Biol. 56, 18–27.

Guarnera, E., Berezovsky, I.N., 2019. Toward comprehensive allosteric control over protein activity. Structure 27, 866–878 e861.

Guarnera, E., Tan, Z.W., Zheng, Z., Berezovsky, I.N., 2017. AlloSigMA: allosteric signaling and mutation analysis server. Bioinformatics 33, 3996–3998.

Gunasekaran, K., Ma, B., Nussinov, R., 2004. Is allostery an intrinsic property of all dynamic proteins? Proteins 57, 433–443.

Hilser, V.J., Thompson, E.B., 2007. Intrinsic disorder as a mechanism to optimize allosteric coupling in proteins. Proc. Natl. Acad. Sci. U. S. A. 104, 8311–8315.

Hinsen, K., Petrescu, A.-J., Dellerue, S., Bellissent-Funel, M.-C., Kneller, G.R., 2000. Harmonicity in slow protein dynamics. Chem. Phys. 261, 25–37.

Huang, Q., Li, M., Lai, L., Liu, Z., 2020. Allostery of multidomain proteins with disordered linkers. Curr. Opin. Struct. Biol. 62, 175–182.

Jacobitz, A.W., Kattke, M.D., Wereszczynski, J., Clubb, R.T., 2017. Sortase transpeptidases: structural biology and catalytic mechanism. Adv. Protein Chem. Struct. Biol. 109, 223–264.

Karginov, A.V., Ding, F., Kota, P., Dokholyan, N.V., Hahn, K.M., 2010. Engineered allosteric activation of kinases in living cells. Nat. Biotechnol. 28, 743–747.

Li, J., White, J.T., Saavedra, H., Wrabl, J.O., Motlagh, H.N., Liu, K., Sowers, J., Schroer, T.A., Thompson, E.B., Hilser, V.J., 2017. Genetically tunable frustration controls allostery in an intrinsically disordered transcription factor. Elife 6.

Ma, B., Tsai, C.J., Haliloglu, T., Nussinov, R., 2011. Dynamic allostery: linkers are not merely flexible. Structure 19, 907–917.

Mitternacht, S., Berezovsky, I.N., 2011. A geometry-based generic predictor for catalytic and allosteric sites. Protein Eng. Des. Sel. 24, 405–409.

Mitternacht, S., Berezovsky, I.N., 2011. Binding leverage as a molecular basis for allosteric regulation. PLoS Comput. Biol. 7, e1002148.

Mitternacht, S., Berezovsky, I.N., 2011. Coherent conformational degrees of freedom as a structural basis for allosteric communication. PLoS Comput. Biol. 7, e1002301.

Monod, J., Changeux, J.P., Jacob, F., 1963. Allosteric proteins and cellular control systems. J. Mol. Biol. 6, 306–329.

Motlagh, H.N., Wrabl, J.O., Li, J., Hilser, V.J., 2014. The ensemble nature of allostery. Nature 508, 331–339.

Naik, M.T., Suree, N., Ilangovan, U., Liew, C.K., Thieu, W., Campbell, D.O., Clemens, J.J., Jung, M.E., Clubb, R.T., 2006. Staphylococcus aureus Sortase A transpeptidase. Calcium promotes sorting signal binding by altering the mobility and structure of an active site loop. J. Biol. Chem. 281, 1817–1826.

Pang, X., Zhou, H.X., 2015. Disorder-to-Order transition of an active-site loop mediates the allosteric activation of sortase A. Biophys. J. 109, 1706–1715.

Papaleo, E., Saladino, G., Lambrughi, M., Lindorff-Larsen, K., Gervasio, F.L., Nussinov, R., 2016. The role of protein loops and linkers in conformational dynamics and allostery. Chem. Rev. 116, 6391–6423.

Saavedra, H.G., Wrabl, J.O., Anderson, J.A., Li, J., Hilser, V.J., 2018. Dynamic allostery can drive cold adaptation in enzymes. Nature 558, 324–328.

Sevcsik, E., Trexler, A.J., Dunn, J.M., Rhoades, E., 2011. Allostery in a disordered protein: oxidative modifications to alpha-synuclein act distally to regulate membrane binding. J. Am. Chem. Soc. 133, 7152–7158.

Tan, Z.W., Tee, W.V., Guarnera, E., Booth, L., 2019. Berezovsky IN: AlloMAPS: allosteric mutation analysis and polymorphism of signaling database. Nucleic Acids Res. 47, D265–D270.

Tan, Z.W., Guarnera, E., Tee, W.V., Berezovsky, I.N., 2020. AlloSigMA 2: paving the way to designing allosteric effectors and to exploring allosteric effects of mutations. Nucleic Acids Res. 48, W116–W124.

Berezovsky, I.N., 2013. Thermodynamics of allostery paves a way to allosteric drugs. Biochim. Biophys. Acta 1834, 830–835.

Berezovsky, I.N., Tumanyan, V.G., Esipova, N.G., 1997. Representation of amino acid sequences in terms of interaction energy in protein globules. FEBS Lett. 418, 43–46.

Tee, W.V., Guarnera, E., Berezovsky, I.N., 2018. Reversing allosteric communication: from detecting allosteric sites to inducing and tuning targeted allosteric response. PLoS Comput. Biol. 14, e1006228.

Tee, W.V., Guarnera, E., Berezovsky, I.N., 2019. On the allosteric effect of nsSNPs and the emerging importance of allosteric polymorphism. J. Mol. Biol. 431, 3933–3942.

Tokuriki, N., Oldfield, C.J., Uversky, V.N., Berezovsky, I.N., Tawfik, D.S., 2009. Do viral proteins possess unique biophysical features? Trends Biochem. Sci. 34, 53–59.

Tsai, C.J., Nussinov, R., 2014. A unified view of "how allostery works. PLoS Comput. Biol. 10, e1003394.

Uversky, V.N., 2002. Natively unfolded proteins: a point where biology waits for physics. Protein Sci. 11, 739–756.

van der Lee, R., Buljan, M., Lang, B., Weatheritt, R.J., Daughdrill, G.W., Dunker, A.K., Fuxreiter, M., Gough, J., Gsponer, J., Jones, D.T., et al., 2014. Classification of intrinsically disordered regions and proteins. Chem. Rev. 114, 6589–6631.

Wang, J., Custer, G., Beckett, D., Matysiak, S., 2017. Long distance modulation of disorder-to-order transitions in protein allostery. Biochemistry 56, 4478–4488.

Wright, P.E., Dyson, H.J., 1999. Intrinsically unstructured proteins: re-assessing the protein structure-function paradigm. J. Mol. Biol. 293, 321–331.

Zong, Y., Bice, T.W., Ton-That, H., Schneewind, O., Narayana, S.V., 2004. Crystal structures of Staphylococcus aureus sortase A and its substrate complex. J. Biol. Chem. 279, 31383–31389.